INTERNATIONAL JOURNAL FOR NUMERICAL METHODS IN FLUIDS
*Int. J. Numer. Meth. Fluids* 2007; **54**:325–332
Published online 30 November 2006 in Wiley InterScience (www.interscience.wiley.com). DOI: 10.1002/fld.1403

# Numerical simulation of thin airfoil stall by using a modified DES approach

Dong Li*, †, ‡

*National Key Laboratory of Aeronautical Fluid Dynamics, School of Aeronautics, Northwestern Polytechnical University, 710072 Xi'an, China*

## SUMMARY

The detached-Eddy simulation (DES) method was applied to calculate pre- and post-stall aerodynamic characteristics of airfoil stall. A discrepancy between numerical and experimental data was observed near the stall regime for the airfoil NACA64$_A$-006 which is a thin airfoil stall type. The reason of this discrepancy and one possible way for improvement of the numerical model are discussed here. It is shown that the use of the Baldwin–Lomax model in the RANS region improves the DES results in this case. If the relevant factors (grid density, time step, turbulence model, etc.) are appropriately taken into account, the DES approach could reliably predict stall aerodynamical characteristics. Copyright © 2006 John Wiley & Sons, Ltd.

Received 17 April 2006; Revised 29 September 2006; Accepted 15 October 2006

KEY WORDS: airfoil; stall; thin airfoil stall; detached-Eddy simulation

## INTRODUCTION

The present study concerns simulation of the flow field around an airfoil at a low speed and a large attack angle. The question is how accurately stall characteristics can be predicted by numerical simulation of highly separated flows.

RANS models [1] can provide accurate results for attached boundary layer flows with minimal grid spacing requirement. However, they often fail in applications to large-scale separated flows that depend on geometry. Large Eddy simulation [1] solves large, energy containing scales by modelling smaller scales. This method requires grid spacing to be prohibitively small. In boundary

*Correspondence to: Dong Li, National Key Laboratory of Aeronautical Fluid Dynamics, School of Aeronautics, Northwestern Polytechnical University, 710072 Xi'an, China.
†E-mail: ldgh@nwpu.edu.cn
‡Associate Professor.

layers, energy containing eddies are so small at high Reynolds numbers that very small stream-wise grid spacing is needed.

Spalart *et al.* [2] proposed the detached-Eddy Simulation (DES) approach that combines the most favourable elements of RANS models with large Eddy simulation. It can be applied to flows at high Reynolds numbers. The DES approach has been successively applied to a delta wing vortex breakdown [3], a supersonic axisymmetric base flow [4], a circular cylinder [5], an airfoil pitch-up [5], and real configurations of several aircrafts [5], etc. It should be noted that the mentioned works focus on practical Reynolds numbers that are close to real flight conditions. In the present work, the DES method is used for the simulation of airfoils stall.

In our prophase study [6], three airfoils with different stall onset mechanisms have been numerically simulated by using the DES approach and RANS approach, which are NACA$63_3$-018 as the trailing-edge stall; NACA$63_1$-012 as the leading-edge stall; NACA64A-006 as the thin airfoil stall [7].

According to results of the numerical simulations [6], for the NACA$63_3$-018 airfoil, the lift loss at the stall regime is caused by the flow separation near the trailing edge. The separation region slowly extends towards upstream as the angle of attack increases. A minor difference is observed between the RANS and DES methods. Thus, for slightly separated flows, the use of RANS models can provide reliable results. In the case of NACA$63_1$-012 airfoil, as the angle of attack increases, the flow suddenly separates in the vicinity of the leading edge. The separation region extends over all the upper surface of the airfoil. This leads to a sudden loss of lift at post-stall regimes. Before the stall, both the RANS and DES methods yield quite reliable results. However, after the stall, the DES results agree much better with experimental data than the RANS results. This indicates the ability of the DES method to handle massively separated flows.

For the NACA64A-006 airfoil, a difference between DES numerical results and experimental data appears before the stall, which becomes severe at stall and post-stall regimes. This occurs due to a bubble that is created near the leading edge. In this study, we discuss several factors (grid density, time step, turbulence model, etc.) that may affect the accuracy of numerical simulations and propose some modifications that can improve numerical results for unsteady regimes of thin airfoils.

## COMPUTATIONAL METHOD

### *Spalart–Allmaras model*

The Spalart–Allmaras one equation model [8] solves a partial differential equation for variable $\tilde{\upsilon}$ which is related to turbulent viscosity

$$\frac{\mathrm{D}\tilde{\upsilon}}{\mathrm{D}t} = c_{b1}[1 - f_{t2}]\tilde{S}\tilde{\upsilon} - \left[c_{w1} f_w - \frac{c_{b1}}{\kappa^2} f_{t2}\right]\left[\frac{\upsilon}{d}\right]^2 + \frac{1}{\sigma}[\nabla \cdot ((\upsilon + \tilde{\upsilon})\nabla\tilde{\upsilon}) + c_{b2}(\nabla\tilde{\upsilon})^2] + f_{t1}\Delta U^2 \quad (1)$$

Then

$$\upsilon_t = \tilde{\upsilon} f_{v1}, \quad f_{v1} = \frac{\chi^3}{\chi^3 + c_{v1}^3}, \quad \chi \equiv \frac{\tilde{\upsilon}}{\upsilon}$$



DOI: 10.1002/fld

$\upsilon$ is the molecular viscosity. The right-hand side of the equation is composed of the production, destruction, diffusion, and transition trip terms, respectively.

*Detached-Eddy simulation*

The DES formulation [2] is based on a modification to the Spalart–Allmaras RANS model such that the model reduces to its RANS formulation near a solid surface and to a subgrid model away from the wall. It takes advantage of both the RANS model in the thin shear layer and the power of LES to resolve geometry-dependent and three-dimensional eddies.

The DES formulation is obtained by replacing the distance to the nearest wall, $d$ by $\tilde{d}$, where $\tilde{d}$ is defined as $\tilde{d} \equiv \min(d, C_{\mathrm{DES}}\Delta)$, where $\Delta$ is the largest one among the distances between the centre of the current cell to the centres of the adjacent cells, and where the value of $C_{\mathrm{DES}}$ is kept constant, $C_{\mathrm{DES}} = 0.65$. The flow field was separated into two parts by length scales, which are called the RANS region and the LES region, respectively.

*Some details of the numerical method*

A 3-D unsteady code was used for the simulation of flow fields of airfoils. The free stream conditions in the non-dimensional form used in the present work are as follows:

$$V_\infty = 0.355$$

$$C = 1.0$$

$$T_{\mathrm{character}} = C / V_\infty = 2.82$$

The pseudotime step [9] is employed for both Navier–Stokes equations and Spalart–Allmaras turbulence equation. The LU-SGS method [10] is used to implicitly discretize the Spalart–Allmaras equation with respect to time. The time steps for physical time are selected as $\Delta t = 0.1$ (3.5% of the time the free stream passes the chord length). Based on numerical experiments, we can see that, $\Delta t$ near the value $\Delta_z * C / V_\infty$ is appropriate for the unsteady simulation of airfoils, which is in line with the advice of Spalart [11]. In the present research work, an explicit local time stepping method is used for inner iterations, 20 inner time steps were used in present work.

From Figure 1, we can see that the average lift (indicated in Figure 1 by square dots) does not get a convergent tendency with respect to the physical time until the physical time $T > 10 \times T_{\mathrm{character}}$, $10 \times T_{\mathrm{character}}$ means $T \approx 30$ (300 physical time steps since $\Delta t = 0.1$ which includes 20 inner iterates for each step). To obtain the convergence, we integrate the lift and average it with respect to physical time to get a convergent value.

Since DES combines a property of LES, the grid density has an important effect. We increase the grid density along the span because the grid size directly affects separation between RANS region and LES region (we define the length scale as the smallest distance from the wall and the grid size, as stated above). $\Delta z = 0.02$ was selected in this study.

Much more details about the former numerical experiences for airfoils stall can be found in Reference [6]. The effect of some factors on numerical results is provided according to Reference [6] in Table I.



DOI: 10.1002/fld

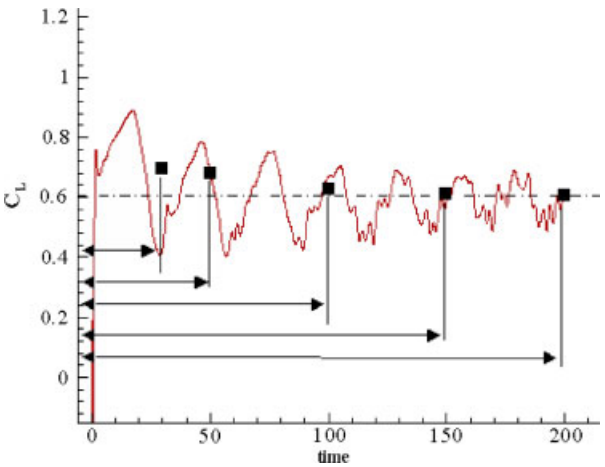


Figure 1. Average lift history.

Table I. The effect of some factors on numerical results.

| Factors | Effect on numerical results |
|---|---|
| Inner iterate | Almost none when >20 |
| Grid density | Improve when increase in span |
| Time step | Almost none when $<3.5\% * T_{\text{character}}$ |
| Transition | Important |
| High-order scheme | To be confident |

## RESULTS AND DISCUSSION

### *Airfoil stall*

The calculations are performed for a Reynolds number of $5.8 \times 10^6$ and a Mach number of 0.3. The grid has 201 points in the stream-wise direction, 81 points normal to the wing, and 50 in the span-wise direction, respectively.

For the case of the NACA$63_1$-012 airfoil, as the attack angle increases, the flow is suddenly separated from the leading edge, in the whole region above the upper surface of the airfoil, leading to lift loss after stall. By using RANS with B-L turbulence model [6], we can only catch the stall angle, but the lift after stall cannot be simulated. However, in the DES method, not only the stall angle can be determined accurately, but also the large separated flow after stall can be simulated in the detached region.

For the case of NACA$63_3$-018 airfoil, the lift loss is caused by flow separation near the trailing edge, which extends rather slowly in the upstream direction as the attack angle increases. No obvious differences are observed between the RANS and DES methods. This means that, for slightly separated flows, use of the RANS approach can provide reliable results.



DOI: 10.1002/fld

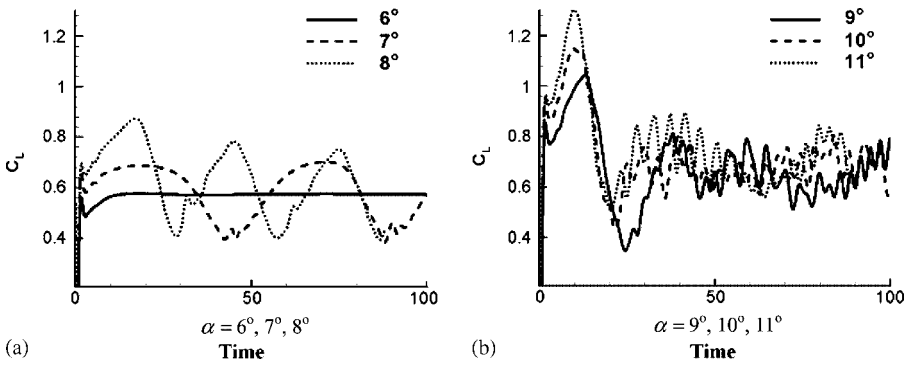


Figure 2. Lift history for attack angles from $\alpha = 6$ to 11° (NACA64A-006 airfoil): (a) $\alpha = 6, 7, 8°$; and (b) $\alpha = 9, 10, 11°$.

For the case of NACA64A-006 airfoil, as the attack angle increases, a separated bubble first appears on the upper surface near the leading edge. The lift increases almost linearly for small attack angles. The first non-linearity in the lift curve appears at $\alpha = 5.27°$, which is due to a bubble produced near the leading edge. Between 6 and 11°, the flow field clearly appears as a periodical phenomenon. At 6°, the flow field is steady and 2-D, at 7°, the flow field becomes unsteady and periodic phenomenon exists, this phenomenon begins to disappear for $\alpha > 8°$, and the flow field shows no specific pattern after this attack angle. The calculations had some difficulties in the case of a thin airfoil stall type, when the bubble becomes unstable and shows periodical variations and extends to full turbulence flow. More details about the numerical analysis can be found in Reference [6]. We focus on the case of a thin airfoil stall in the present work to find a way to improve the numerical results.

*Thin airfoil stall simulation*

The NACA64A-006 with thin airfoil stall is selected for this study.

For this type of airfoil, as the attack angle increases, first a separated bubble appears on the upper surface near the leading edge. This occurs at $\alpha \approx 5.27°$ and leads to a non-linearity in the lift curve. The lift time history is shown in Figures 2(a) and (b) for the attack angles $\alpha = 6, 7, 8°$, and 9, 10, 11°, respectively.

*A modified DES approach*

The effect of the turbulence model of the wall-adjacent flow was taken into account in the present work. We examined a different turbulence model in the RANS region, to be exact—the Baldwin–Lomax model, which is known to give very good results for attached wall confined flows. Thus, the turbulence model to be used is a modified DES approach, where the Spalart–Allmaras equation with the modified wall distance parameter $\tilde{d}$ is used for the LES region, while the Baldwin–Lomax model is utilized in the RANS region.

The calculations are performed with the mesh size $\Delta z = 0.02$. Figure 3 displays the flow field for four different instants at $\alpha = 8°$ as a typical state near the stall. The bubble near the leading edge is not stable in this case; it breaks into smaller bubbles, and then the flow almost reattaches



DOI: 10.1002/fld

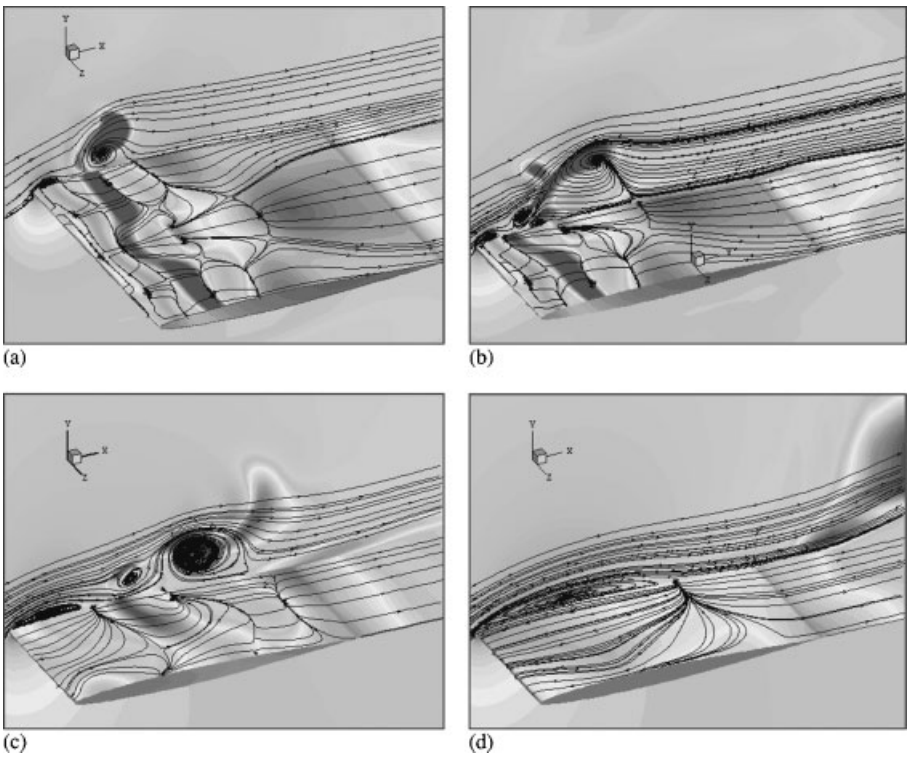


Figure 3. Pressure contours and streamlines at different instants for $\alpha = 8^\circ$ (NACA64A-006): (a) $t = t_1$; (b) $t = t_2$; (c) $t = t_3$; and (d) $t = t_4$.

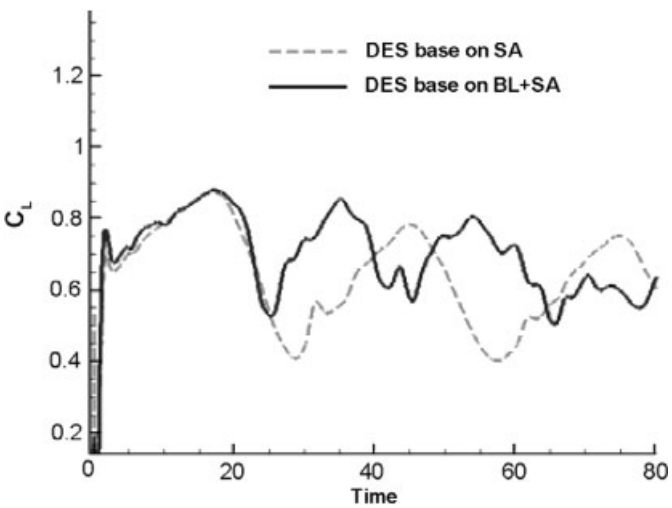


Figure 4. Effect of the model used in the RANS region.



DOI: 10.1002/fld

Table II. Effect of the RANS model on averaged coefficients.

| $\alpha = 8^\circ$ | $C_L$ | $C_D$ | $C_M$ |
|---|---|---|---|
| EXP | 0.76 | 0.098 | −0.03 |
| DES (SA) | 0.604 | 0.085 | −0.047 |
| DES (BL + SA) | 0.705 | 0.100 | −0.066 |

*Note*: BL, Baldwin–Lomax; SA, Spalart–Allmaras.

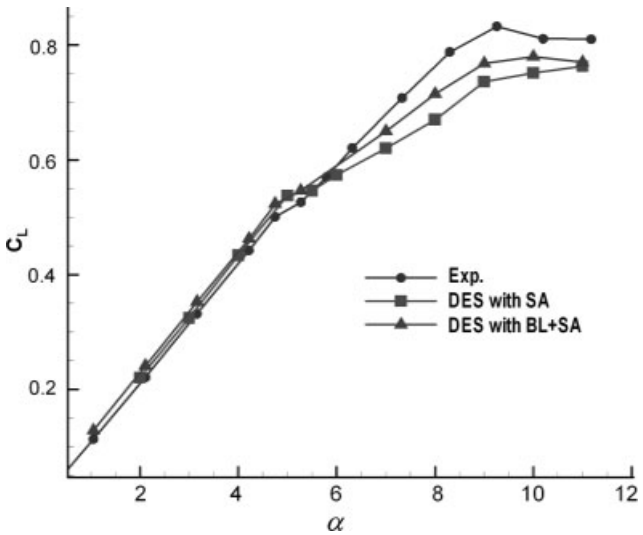


Figure 5. Lift *vs* attack angle for NACA64A-006 airfoil. SA, Spalart–Allmaras; BL, Baldwin–Lomax.

the upper surface. Later the flow separation begins again with the formation of a new leading-edge bubble. This process is periodically repeated.

The lift time histories for the attack angle $\alpha = 8^\circ$ are presented in Figure 4, which correspond to the DES model based either entirely on the Spalart–Allmaras model or on the Spalart–Allmaras model implemented with the Baldwin–Lomax model for the RANS region, respectively.

As can be seen from Figure 4, the lift time histories given by Spalart–Allmaras and Spalart–Allmaras + Baldwin–Lomax model deviate from each other after some initial time. The minimal lift achieved in the Baldwin–Lomax + Spalart–Allmaras simulation appears to be larger than that in the Spalart–Allmaras simulation. In Table II we list the values of the time-averaged lift, drag and momentum coefficients in the Spalart–Allmaras and Spalart–Allmaras + Baldwin–Lomax simulations. One can see that using the Baldwin–Lomax model instead of Spalart–Allmaras model in the RANS region leads to higher averaged values, which agree much better with the experimental data.

In Figure 5 we show the improvement that can be achieved in the DES lift prediction by means of foregoing modification.



DOI: 10.1002/fld

## CONCLUSIONS

For the airfoil NACA64A-006, the bubble is destabilized as the angle of attack is increased and the flow becomes unsteady and highly turbulent. Refining the grid in the spanwise direction affects the numerical results in this case and shows the trend from a quasi-periodical to a turbulent behaviour; however, a discrepancy between numerical and experimental data was still observed near the stall regime. It has been shown that the use of the Baldwin–Lomax model in the RANS region improves the DES results further. Taking these factors into consideration, the DES approach could reliably predict stall aerodynamical characteristics.

## NOMENCLATURE

| | |
|---|---|
| $\upsilon$ | molecular viscosity coefficient |
| $\tilde{\upsilon}$ | turbulence model variable |
| $\upsilon_t$ | turbulent viscosity coefficient |
| $\Delta t$ | time step |
| $\tilde{d}$ | length scale |
| $d$ | wall distance |
| $\Delta$ | local grid size |
| $M_\infty$ | free-stream Mach number |
| $C$ | airfoil chord length |
| $\alpha$ | angle of attack |
| $C_L$ | lift coefficient |
| $C_D$ | drag coefficient |
| $C_M$ | momentum coefficient |

## REFERENCES

1. Charles GS. Turbulence modeling for time-dependent RANS and VLES: a review. *AIAA Paper 97-2051*, 1997.
2. Spalart PR, Jou W-H, Strelets M, Allmaras SR. Comments on the feasibility of LES for wings, and on a hybrid RANS/LES approach. *First AFOESR International Conference on DNS/LES*, Ruston, LA; In *Advances in DES/LES*, Liu C, Liu Z (eds). Greyden Press: Columbus, OH, 1997.
3. Morton S, Forsythe JR, Mitchell A, Hajek D. DES and RANS simulations of delta wing vortical flows. *AIAA Paper 2002-0587*, 2002.
4. Forsythe JR, Hoffmann KA, Squires KD. Detached-Eddy simulation with compressibility corrections applied to a supersonic axisymmetric base flow. *AIAA Paper 02-0586*, 2002.
5. Squires KD, Forsythe JR, Morton SA, Strang WZ, Wurzler KE, Tomaro RF, Grismer MJ, Spalart PR. Progress on detached-Eddy simulation of massively separated flows. *AIAA Paper 2002-1021*, 2002.
6. Dong L, Men'shov I, Nakamura Y. Numerical prediction for airfoil stall. *ICAS2004*, Yokohama, Japan, September 2004.
7. George B, Donald E. Examples of three representative types of airfoil section stall at low speed. *NACA Technical Report*, *TN-2502*, 1951.
8. Spalart PR, Allmaras SR. A one-equation turbulence model for aerodynamic flows. *AIAA Paper 92-0439*, 1992.
9. Jameson A. Time dependent calculations using multigrid, with applications to unsteady flows past airfoils and wings. *AIAA Paper 91-1596*, June 1991.
10. Men'shov I, Nakamura Y. On implicit Godunov method with exactly linearized numerical flux. *Computers and Fluids* 2000; **29**(6):695–616.
11. Spalart PR. Young-person's guide to detached-Eddy simulation grids. *NASA/CR-2001-211032*, July 2001.



DOI: 10.1002/fld